Calibration of an Optomechanical Image Derotator with a 6-Axes Parallel Kinematics Using Image Processing Algorithms

Benjamin Rohloff
Institute of Measurement and Automatic Control, Leibniz Universität Hannover
Nienburger Str. 17, 30167 Hannover, Germany
E-Mail: benjamin.rohloff@imr.uni-hannover.de

Abstract

The use of an optomechanical image derotator for the analysis of rotating objects requires a calibration with respect to the position of the derotator compared to the measured object. The goal of the calibration is to position the optical axis of the derotator coaxially to the rotational axis of the measured object. If this is not the case, the use of optical measurement methods is made more difficult by a movement of the optical image of the derotator. In the present work, a mathematical model of the optomechanical image derotator is presented, which was developed at the Institute of Measurement and Automatic Control. On the basis of the model, different effects are studied which arise from an incorrect calibration of the overall system and of an incorrect adjustment of the mirror system. Based on these investigations, a calibration strategy is developed and critically discussed in terms of its usability in the experiment.

Introduction

The investigation of rotating objects during operation is still essential for a comprehensive understanding of the system behavior. If measuring devices are implemented, which are in direct contact with the measured object, it often incurs with a significant change in its physical properties, which can not be neglected in the evaluation of the measurement results. The use of non-contact methods such as Laser Doppler Vibrometry is problematic, cause an adaptation to the rotation is necessary. For this purpose an optomechanical image derotator is available, which transforms the stationary laboratory coordinate system in the rotating coordinate system of the object, whereby the use of optical measuring methods is feasible. In [2] is achieved a fundamental understanding of the occurrence of slip in rolling bearings with a derotator based on a rotating dove prism and a high-speed camera. The investigations are supplemented by measurements with a Laser Doppler Vibrometer at a cut-off wheel. This approach is taken by [3] and [4] and used for the identification of the vibrational modes of a saw blade. However, when using a dove prism, some effects can not be ignored. [5] discribes the aberrations, which usually occur in lenses. Moreover, a dove prism can not used for thermographic analyses. In vibration analyses with a Laser Doppler Vibrometer, there is a modulation of the intensity of polarized light, which prevents reflection on the prism base surface, so that a part of the light emerges from the glass. These artifacts can be avoided with a new concept. This is a rotating mirror body assembly, called mirror-dove [5]. Structure and function are described in detail in the following chapter. With such a derotator, [6] makes vibration tests on a model of a blisk, identifying the effects of phenomena such as centrifugal stiffening of the blade.

Derotator Experimental Equipment

The core element of the entire experimental set-up is the rotating mirror body assembly that has already been mentioned in the previous chapter. The basic operation is shown in figure 1.

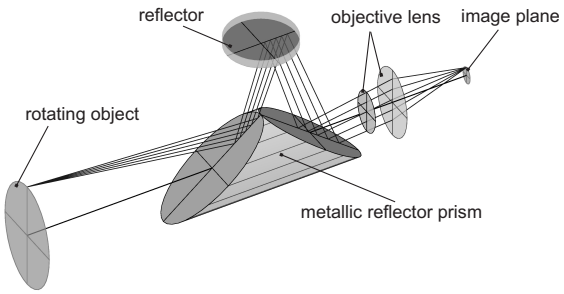

Figure 1: Key element of the optomechanical image derotator, ©IMR

The light rays emanating from a rotating object are deflected by the co-rotating mirror-dove three times and can be displayed by a lens in an image plane. It is necessary that the speed of the mirror corresponds to half of the speed of the measured object. The derotational effect is illustrated by the principle of a rotator. Figure 2 shows the rotation of an effective reflection plane by the angle α.

The result is a rotation of the vertical axis of any object by the angle $2 \times \alpha$. This means that a rotation of the effective reflection plane by the angle α is necessary to derotate the vertical axis of the object. If this effect is transferred to rotating objects, it is clear that the mirror body arrangement in figure 1 has to rotate with respect to the measured object at half the angular speed. Thereby, the viewer is transformed in the rotating coordinate system and the object is perceived standing. The mirror-dove is installed in a hollow shaft motor, which allows speeds up to 12.000 rpm, so that measured ob-

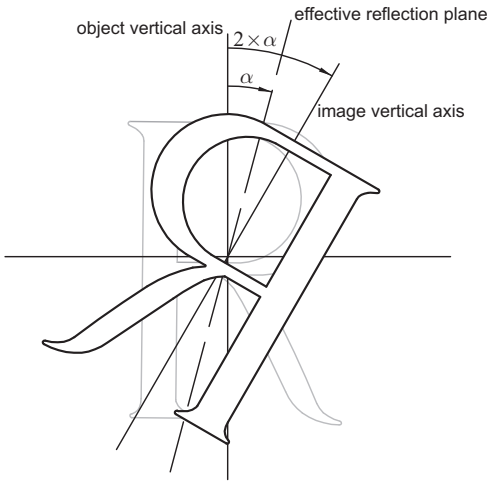

Figure 2: Functional prinziple of a rotator, ©IMR

jekts can be analyzed up to 24.000 rpm. The complete experimental setup can be found in figure 3.

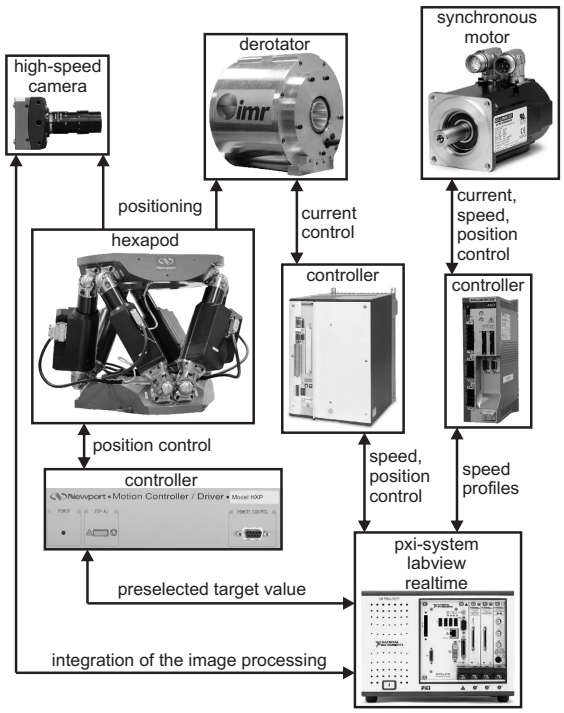

Figure 3: Experimental setup, ©IMR

The current work is concerned with the integration of all components into a complete system that is monitored and controlled via a PXI-System from National Instruments. Speed and position control of the derotator and the target motor should be computed on the system so that it is possible to implement advanced control concepts. It should be possible to calibrate the derotator to the object automatically. The calibration is necessary, because the optical axes of derotator and measured object must be coaxial. If this is not the case, the optical imaging is disturbed by movements. The calibration is based on an analysis of the image informations which are received from the high-speed camera. First steps in this direction have already been completed and will be presented in the following chapter.

Modelling of the Optomechanical Image Derotator

The assumptions of geometrical optics are valid for the mathematical modeling of the optical imaging. This allows the consideration of light bundles, consisting of light rays, whereas effects of wave optics (e.g. diffraction) can be neglected. Under this simplification, it is necessary for the diameter of the light beam to meet the condition $D > 10\mu m$ when an average wavelength in the visible region $\lambda = 500nm$ is present.

Furthermore, three coordinate systems are required for the modeling. An inertial laboratory coordinate system with the index i, which origin is located in the intersection of the rotational axis of the object with the object plane.

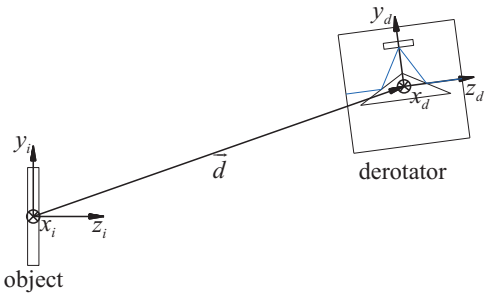

Figure 4: Object and derotator coordinate system, ©IMR

The second coordinate system with the index d refers to the rotating derotator, so that its position will be described in the inertial coordinate system. Both coordinate systems can be found in figure 4. A defined point in the object space

$$\vec{Q}_i = \begin{pmatrix} x_i \\ y_i \\ z_i \end{pmatrix}$$

is thus represented in the coordinate system of the derotator by

$$\vec{Q}_d = \begin{pmatrix} x_d \\ y_d \\ z_d \end{pmatrix}.$$

By further transformations resulting from the mirror arrangement and the camera, which is connected to the derotator, the object point

$$\vec{B}_b = \begin{pmatrix} x_b \\ y_b \\ 0 \end{pmatrix}$$

is displayed in the image space. For the transformation of the image point in the coordinate system of the derotator a translation vector

$$\vec{d} = \begin{pmatrix} d_x \\ d_y \\ d_z \end{pmatrix},$$

the rotation matrix around the x-axis with the angle α

$$R_x = \begin{pmatrix} 1 & 0 & 0 \\ 0 & \cos\alpha & \sin\alpha \\ 0 & -\sin\alpha & \cos\alpha \end{pmatrix},$$

the rotation matrix around the y-axis with the angle β

$$R_y = \begin{pmatrix} \cos\beta & 0 & -\sin\beta \\ 0 & 1 & 0 \\ \sin\beta & 0 & \cos\beta \end{pmatrix}$$

and the rotation matrix around the z-axis

$$R_z = \begin{pmatrix} \cos\gamma & \sin\gamma & 0 \\ -\sin\gamma & \cos\gamma & 0 \\ 0 & 0 & 1 \end{pmatrix}$$

with the angle γ are necessary. All rotation matrices are defined by roll-pitch-yaw. In order to model the rotation of the mirror system, a further rotation matrix

$$R_{rot} = \begin{pmatrix} \cos\delta & \sin\delta & 0 \\ -\sin\delta & \cos\delta & 0 \\ 0 & 0 & 1 \end{pmatrix}$$

around the z-axis with the angle δ is required. Using the common rotation matrix

$$R_{id} = R_{rot} \cdot R_z \cdot R_y \cdot R_x$$

the point $\vec{Q}_i$ in the coordinate system of the derotator can be represented by

$$\vec{Q}_d = R_{id}\left(\vec{Q}_i - \vec{d}\right).$$

With the help of simple methods of analytic geometry, the total beam path

$$\vec{B}_d = \vec{Q}_d + t_0\vec{b}_0 + t_1\vec{b}_1 + t_2\vec{b}_2 + t_3\vec{b}_3 + t_4\vec{b}_4$$

can be determined, based on a simplified camera model with a so-called thin lens. The total beam path is shown in figure 5.

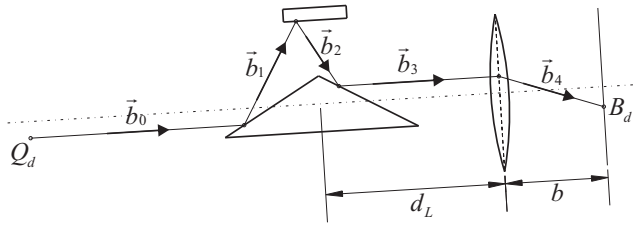

Figure 5: Beam extending through the derotator and an ideal lens, ©IMR

Subsequently, the image point $\vec{B}_d$ is moved to the coordinate origin by the vector

$$\vec{d}_k = \begin{pmatrix} 0 \\ 0 \\ d_L + b \end{pmatrix}$$

and the rotation is removed

$$\vec{B}_b = R_{rot}^T\left(\vec{B}_d - \vec{d}_k\right),$$

because the camera is not co-rotating with the mirror system. The index b is not a sign of another coordinate system but an indication of the image plane in the camera. The optical image of a point having the coordinates x_i, y_i can determined by

$$\begin{aligned} x_b = (&2x_i\cos\beta + 2y_i\sin\alpha\sin\beta - 2d_x\cos\beta \ldots \\ &- 2d_y\sin\alpha\sin\beta + 2d_z\cos\alpha\sin\beta)\cos^2\delta \ldots \\ &+ (y_i\cos\alpha - d_y\cos\alpha - d_z\sin\alpha)\sin 2\delta \ldots \\ &- x_i\cos\beta - y_i\sin\alpha\sin\beta + d_x\cos\beta \ldots \\ &+ d_y\sin\alpha\sin\beta - d_z\cos\alpha\sin\beta \end{aligned} \quad (1)$$

and

$$\begin{aligned} y_b = (&-2y_i\cos\alpha + 2d_y\cos\alpha + 2d_z\sin\alpha)\cos^2\delta \ldots \\ &+ (x_i\cos\beta + y_i\sin\alpha\sin\beta - d_x\cos\beta \ldots \\ &- d_y\sin\alpha\sin\beta + d_z\cos\alpha\sin\beta)\sin 2\delta \ldots \\ &+ y_i\cos\alpha - d_y\cos\alpha - d_z\sin\alpha. \end{aligned} \quad (2)$$

A tilting of the z_d-axis is not considered, because it can be represented by a rotation of the mirror system, so that $\gamma = 0$ applies. These two equations form the basis of all further considerations.

Ideal Optical Imaging

An ideal optical imaging can be expected, when the derotator against the measured object is not shifted ($d_x = d_y = 0$) and not tilted ($\alpha = \beta = 0$). A rotating point at the angular speed ω_Q

$$\vec{Q}_i = \begin{pmatrix} r\cos(\varphi_0 + \omega_Q t) \\ r\sin(\varphi_0 + \omega_Q t) \end{pmatrix}, \quad (3)$$

which is displaced about the angle φ_0 compared to the derotator, is descirbed by simplifying the equations 1 and 2

$$\vec{B}_b = \begin{pmatrix} r\cos(\varphi_0) \\ -r\sin(\varphi_0) \end{pmatrix} \quad (4)$$

by taking into account the coupling condition $\omega_D = \frac{1}{2}\omega_Q$ The position of this point in the image plane is stationary.

Image Movement Caused by a Parallel Shift

The first possible deviation from an ideal calibration is a parallel shift of the optical axis of the derotator to the rotational axis of the measured object, so that the condition $\alpha = \beta = 0$ applies. Based on equation 3, the equations 1 and 2 can be simplified to

$$x_b = r - d_x\cos 2\delta - d_y\sin 2\delta$$

and

$$y_b = -d_x\sin 2\delta + d_y\cos 2\delta,$$

wherein the phase shift φ_0 is not included.

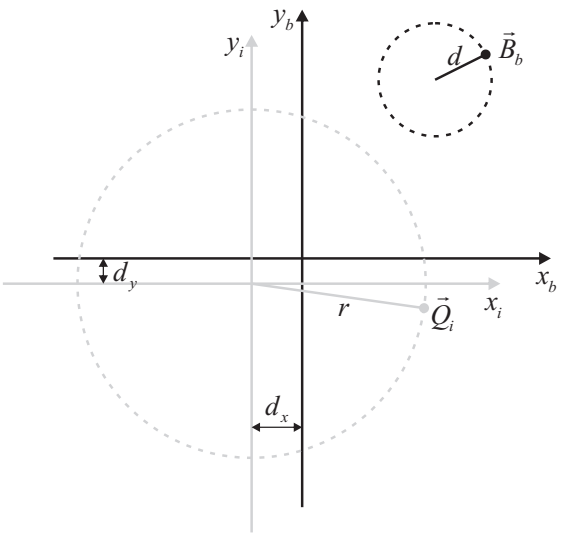

Figure 6: Movement of the optical imaging caused by a parallel shift of the optical axis, ©IMR

Figure 6 shows, that the imaged point moves on a circular track of the radius

$$d = \sqrt{d_x^2 + d_y^2}.$$

The angle corresponds to twice the rotation angle of the derotator. These results are consistent with studies by [1] on a derotator based on a different concept.

Association between Tiltings and Shiftings

The connection between shiftings and tiltings can be investigated assuming that the derotator is calibrated optimally in one dimension. The optical axis is thus either in the x_i, z_i-plane of the object coordinate system, or in the y_i, z_i-plane. In the first case, the conditions are $d_y = 0$ and $\alpha = 0$. If a point is in the origin of the object coordinate system, the imaging equations 1 and 2 can be transformed to

$$\frac{d_x}{d_z} = \tan\beta.$$

It can be seen, that tilts (here the angle β) can be replaced by shifts (d_x and d_z). If the optical axis passes through the y_i, z_i-plane, an equivalent connection is

$$\frac{d_y}{d_z} = -\tan\alpha.$$

From an ideal calibration state shifts can be compensated by tilts. The derotator would provide a perfect optical image as it would be oriented to the object center, even if the optical axis and the rotational axis of the measured object are not coaxial. [1] describes this situation as adjusted state of tune. Further studies adress the prevention of this condition.

Implementation of an Adjusting Error

The real derotator is subject to normal manufacturing tolerances, so it must be assumed that the rotating mirror assembly can not be perfectly aligned and a residual deviation exists. For this reason, an adjusting error is modeled, which results from the misalignment of the mirror system. Figure 7

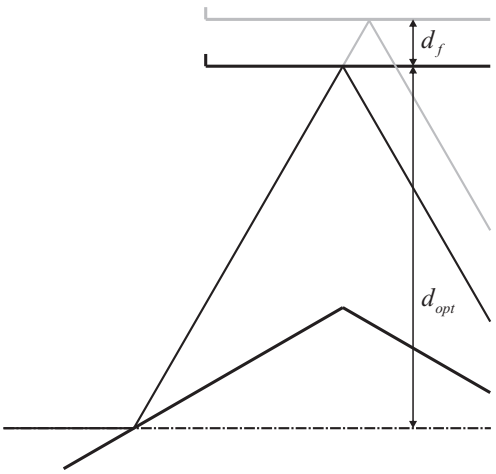

Figure 7: Movement of the optical imaging caused by a parallel shift of the optical axis, ©IMR

shows the eccentrically rotating mirror above its optimum position. The imaging equations 1 and 2 can transformed to

$$\begin{aligned} x_b = (&2x_i\cos\beta + 2y_i\sin\alpha\sin\beta - 2d_x\cos\beta \ldots \\ &- 2d_y\sin\alpha\sin\beta + 2d_z\cos\alpha\sin\beta)\cos^2\delta \ldots \\ &+ (y_i\cos\alpha - d_y\cos\alpha - d_z\sin\alpha)\sin 2\delta \ldots \\ &+ d_f\sin\delta - x_i\cos\beta - y_i\sin\alpha\sin\beta \ldots \\ &+ d_x\cos\beta + d_y\sin\alpha\sin\beta - d_z\cos\alpha\sin\beta \end{aligned} \quad (5)$$

and

$$\begin{aligned} y_b = (&-2y_i\cos\alpha + 2d_y\cos\alpha + 2d_z\sin\alpha)\cos^2\delta \ldots \\ &+ (x_i\cos\beta + y_i\sin\alpha\sin\beta - d_x\cos\beta \ldots \\ &- d_y\sin\alpha\sin\beta + d_z\cos\alpha\sin\beta)\sin 2\delta \ldots \\ &- d_f\cos\delta + y_i\cos\alpha - d_y\cos\alpha - d_z\sin\alpha. \end{aligned} \quad (6)$$

If only the adjusting error is considered ($d_x = d_y = \alpha = \beta$), these equations can simplified to

$$x_b = r\cos\varphi_0 + d_f\sin\delta$$

and

$$y_b = -r\sin\varphi_0 - d_f\cos\delta.$$

Again a rotating point on a circular path is assumed in accordance with equation 3. The result is a derotated, stationary image like in equation 4. However, a circular movement is superimposed on the radius d_f. The angle corresponds only to the simple rotational angle of the derotator.

Combination of Derotator Error and Calibration Error

Based on the assumption, that the distance between the derotator and the measured object is much greater than the miscalibration ($d_z \gg d_x, d_y$), the equations 5 and 6 can be converted to

$$x_b = r\cos\varphi_0 - d_x\cos 2\delta - d_y\sin 2\delta + d_f\sin\delta$$

and

$$y_b = -r\sin\varphi_0 - d_x\sin 2\delta + d_y\cos 2\delta - d_f\cos\delta,$$

using $\cos(\alpha,\beta) \approx 1$ and $\sin(\alpha,\beta) \approx 0$. Again a point in accordance with equation 3 is assumed. Transferred into matrix form

$$\vec{B}_b = \underbrace{\begin{pmatrix} r\cos\varphi_0 \\ -r\sin\varphi_0 \end{pmatrix}}_{I} + \underbrace{\begin{pmatrix} \cos 2\delta & \sin 2\delta \\ \sin 2\delta & -\cos 2\delta \end{pmatrix} \cdot \begin{pmatrix} -d_x \\ -d_y \end{pmatrix}}_{II} + \underbrace{\begin{pmatrix} d_f\sin\delta \\ -d_f\cos\delta \end{pmatrix}}_{III}$$

the movement can be split in the stationary optical image (I), the influence of a displacement of d_x, d_y (II) and the impact of an adjusting error (III). Only the units (II) and (III) generate a movement of the image. Both are independent of the measured object point coordinates so that it can be concluded that any point can be considered. The movement is solely a function of the rotation angle of the derotator δ and of the parallel shiftings d_x, d_y, respectively the adjusting error. It resembles a so-called Limacon of Pascal, shown in figure 8.

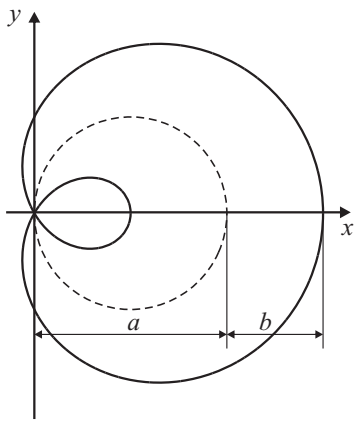

Figure 8: Limacon of Pascal, ©IMR

This special case of a general conchoid can be calculated by

$$x = a\cos^2\varphi + b\cos\varphi \tag{7}$$

and

$$y = a\cos\varphi\sin\varphi + b\sin\varphi \tag{8}$$

using $a, b > 0$ and $0 \le \varphi < 2\pi$. The direct relationship between the optical image $\vec{B}_b$ and the Limacon of Pascal can be established, if $\vec{B}_b$ will be reduced by the stationary component

$$\vec{c} = \begin{pmatrix} r\cos\varphi_0 \\ -r\sin\varphi_0 \end{pmatrix}$$

and the translation $\vec{d}$. Thereafter, the shift of the optical axis of the derotator to the rotational axis of the measured object is replaced by $d_x = d\cos\gamma$ and $d_y = d\sin\gamma$ using $d = \left|\vec{d}\right|$. The rotation of the angle γ is eliminated with the rotation matrix

$$R_\gamma = \begin{pmatrix} \cos -\gamma & -\sin -\gamma \\ \sin -\gamma & \cos -\gamma \end{pmatrix} = \begin{pmatrix} \cos\gamma & \sin\gamma \\ -\sin\gamma & \cos\gamma \end{pmatrix}.$$

The new image can calculated with

$$\vec{B}_n = R_\gamma\left(\vec{B}_b - \vec{c} - \vec{d}\right).$$

After some trigonometric transformations and by using the substitution $(\delta - \gamma) = \left(\varphi + \frac{\pi}{2}\right)$ this image can transformed to

$$x_n = 2d\cos^2\varphi + d_f\cos\varphi \tag{9}$$

and

$$y_n = 2d\cos\varphi\sin\varphi + d_f\sin\varphi. \tag{10}$$

This description corresponds to the parametric representation of the Limacon of Pascal according to the equations 7 und 8 with the parameters $a = 2d$ and $b = d_f$.

Model-Based Calibration Strategies

The previous mathematical considerations lead to the same results as the ones derived in [1] for a different derotator. Thus, the same conclusions regarding the direction of the Limacon of Pascal can be drawn. According to [1] the symmetry axis of the Limacon of Pascal is aligned to the plane, which is defined by the rotational axis of the measured object and the optical axis of the derotator. Figure 9 shows the direction of the Limacon of Pascal in the stationary laboratory coordinate system.

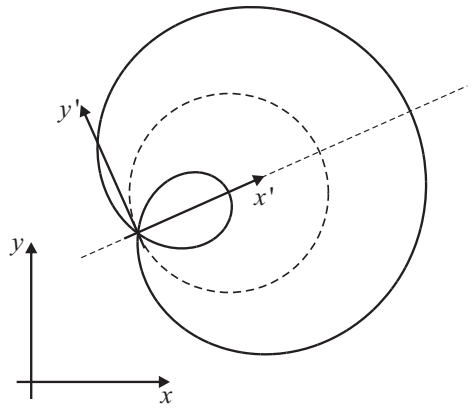

Figure 9: Orientation of the Limacon of Pascal, ©IMR

The characteristics of this curve results from an offset of the rotational axis of the measured object and the optical axis of the derotator and the occurrence of an adjusting error. If the derotator is shifted by d in the direction of the symmetry axis of the Limacon of Pascal using the parallel kinematics, the influence of the calibration error can be eliminated on the optical image. Nevertheless a circular motion will occur, which has its origin in an incorrect adjustment. It is not expected that this problem can be avoided entirely because the derotator is a real system, where it comes to manufacturing tolerances. Moreover, at this point the adjusted state of tune already described above must be discussed again. The determined calibration strategy can not ensure that this condition is avoided because it can not distinguish between shifts and tilts of the rotational axis of the measured object relative to the optical axis of the derotator. Therefore, further studies are needed to resolve this problem besides an experimental validation of the calibration strategy.

References

[1] Miesner, J.: Beitrag zur kontinuierlichen interferometrischen Untersuchung der Eigenschwingformen rotierender Bauteile. Carl von Ossietzky Universität Oldenburg Dissertation 2004

[2] Reithmeier, E.; Mirzaei, S.; Kasyanenko, N.: Optical vibration and deviation measurement of rotating machine parts. Optoelectronics Letters, Vol. 4, No. 1, S. 45-48, 2008

[3] Mirzaei, S.; Rahlves, M.; Fahlbusch, T.; Reithmeier, E.: Application of an Optomechanical Image Derotator for Measuring Vibration and Deformation of Rotating Objects. Proceedings Optimess, 2009

[4] Rahlves, M.; Mirzaei, S.; Fahlbusch, T.; Reithmeier, E.: In-plane and out-of-plane deformation and vibration measurement using an optomechanical image derotator. Proc. SPIE 'Optical Inspection and Metrology for Non-Optics Industries' (Optics and Photonics) 7432, 2009

[5] Mirzaei, S.: Entwicklung und Erprobung der Bildderotator-Messtechnik am Beispiel der Schlupfmessung von Wälzlagern. Leibniz Universität Hannover Dissertation 2011

[6] Rohloff, B.; Schwarzendahl, S.; Wallaschek, J.; Reithmeier, E.(2013): Schwingungsanalyse von rotierenden Objekten mit einem optomechniaschen Bildderotator, 3. VDI-Fachtagung Schwingungsanalyse & Identifikation, Leonberg, S. 203-211, ISBN 978-3-18-092191-4